Natural Resources for Human Health
eISSN: 2583-1194

Original Research

**Received** 11 July 2026
**Revised** 15 Aug 2026
**Accepted** 30 Aug 2026

Natural Resources for Human Health 2026, Vol. 6 (18s): 1056–1065

**KEYWORDS**:
Brain Tumor Segmentation, WFCM (Weighted Fuzzy C-means), EPO (Emperor Penguin Optimization) , Bra TS Data sequence, Dice Score and Medical Image Analysis

# Multi-Modal Deep Learning for Brain Tumor Prognosis Prediction Using MRI and Clinical Data

Vipin Kumar[1], Dr.Naveen Kumar Singh[2], Tarachand Verma[3], Vinay Dwivedi[4], Rahul Dev Singh[5]

[1]Department of Computer Science and Engineering, HRIT University, India
Email: vksnp111@gmail.com
[2]Department of Computer Science and Engineering, HRIT University, India
[3]Department of Computer Science and Engineering, IILM University, Greater Noida, India
Email: trchnd22@gmail.com
[4]Department of Computer Science and Engineering, Galgotias University, Greater Noida, India
Email: vinaydwvd@gmail.com
[5]Department of Computer Science and Engineering, CGC Jhanjeri, Mohali, India
Email: rahul86.dev@gmail.com

**ABSTRACT:** Medical imaging segmentation serves as a critical preprocessing step that enables reliable diagnosis, quantitative analysis, and treatment planning. Its clinical application spans tissue differentiation, tumor detection, lesion sizing, and cellular analysis, among others. FCM (Fuzzy C-Means) clustering is a commonly adopted segmentation approach, yet its accuracy degrades in noisy environment. To address this shortcoming, Weighted Fuzzy C-Means (WFCM) incorporates intensity patterns from surrounding pixels, producing more stable and noise-resilient segmentation outcomes. This work further enhances segmentation performance by coupling WFCM with the EPO (Emperor Penguin Optimizer), a bio-inspired meta-heuristic tool that emulates the collective huddling behavior strategy of penguins (emperor) to achieve a most suited trade-off between exploration with exploitation in the search space. The suggested hybrid EPO-WFCM framework is applied to brain MRI data for tumor identification, with its performance validated against ground-truth images using recognized evaluation metrics - offering clinicians a faster, more dependable diagnostic tool for treatment planning.

## 1. INTRODUCTION

Modern diagnostic healthcare relies heavily on medical imaging to reveal vital anatomical and pathological insights within the human body. Recent advances in technology, particularly artificial intelligence, have transformed this field, enabling more precise and efficient analysis. Among available modalities, CT (Computed Tomography) and MRI (Magnetic Resonance Imaging) remain the most widely employed approach for evaluating with diagnosing a broad range of medical conditions. A tumor in the body represents abnormal and uncontrolled having accurate imaging-based assessment.

Dhiman G.et al.,(2018) introduced Emperor Penguin Optimizer (EPO), a bio-inspired metaheuristic AI-based algorithms penguin huddling dynamics, validated on key role and engineering problems, describing competitive convergence, robustness, and optimization efficiency. Chen D. et al.,(2018) examined high-resolution multispectral satellite imagery integrated with optimized vegetation indices, wrapper-based feature selection, and machine-learning classifiers enables

accurate wheat-rust mapping, supporting scalable disease surveillance, early detection, and precision agricultural management. Deng L. et al.,(2018) investigated biologically inspired pest-recognition framework having saliency detection, SIFT-enhanced HMAX, sparse coding, and texture descriptors with SVM, enabling robust insect identification under complex environmental conditions. Deng X. et al.,(2019) studied hyperspectral reflectance-based machine with non-destructive framework for early citrus HLB detection, integrating entropy-distance and sequential backward selection for informative band extraction, dimensionality reduction, and reliable discrimination of healthy, symptomatic, and asymptomatic infections. Dhingra G. et al.,(2019) integrated neutrosophic-logic-based leaf segmentation framework having texture, color, histogram, and disease-region feature with machine-learning classifiers, achieving 98.4% accuracy and enabling reliable, automated identification of healthy and diseased leaves. Chen C.J. et al.,(2020) integrated intelligent AIoT framework with YOLOv3-based pest detection, environmental sensing, and LSTM forecasting to enable real-time, precise pest monitoring, supporting targeted pesticide application, reduced crop losses, and sustainable agriculture Barman U. et al.,(2020) employed smartphone-enabled deep-learning framework with MobileNet and Self-Structured CNN (SSCNN) having automated citrus disease identification, with SSCNN offering superior classification accuracy, computational efficiency, and cost-effective deployment for accessible precision agriculture. Ramaraj K. et al.,(2022a) discussed ABC-ScARKFCM model by introducing optimization of artificial bee colony with spatially constrained kernel fuzzy C-means, enhancing MRA/MRI segmentation, convergence, and intensity handling, achieving 87.89% Dice, 98.9% sensitivity, and 98.98% specificity. Ramaraj K. et al.,(2023) studied hybrid MLDA-NRBFNN framework that accurately classifies osteoporosis using bone mineral density data, achieving 97.5% accuracy while addressing high-dimensional limitations, supporting early diagnosis, clinical assessment, and improved bone-health management.

Jamazi C.et al.,(2024) integrated MAO-Kmeans framework with adaptive selection and Cauchy mutation having Aquila Optimization by enabling robust cluster-center identification, enhanced convergence, and accurate MRI brain-tumor segmentation on BraTS 2020. Pandey S. et al.,(2024) examined MPUnet that enables robust multi-planar MRI tumor segmentation across diverse datasets, improving tumor-core delineation through advanced preprocessing, multimodal integration, and optimized architecture. Sakli M. et al.,(2024) presented an advanced deep-learning model that formulated precise, automated, and noninvasive brain-tumor segmentation from multimodal MRI, achieving exceptional performance with over 99.3% accuracy, sensitivity, specificity, precision, and 85.69% IoU. Qiu C.et al.,(2024) introduced a robust multiscale Transformer framework for incomplete multimodal MRI, exploiting intermodal correlations and hierarchical features to accommodate missing sequences, enhance tumor delineation, and achieve state-of-the-art BraTS 2018 performance. Yu H.et al.,(2024) introduced FW-S-PFCM model with adaptive feature of weighting and suppressed competitive learning to resolve feature imbalance, noisy-center overlap, and initialization sensitivity, delivering robust clustering, improved segmentation accuracy, and enhanced computational stability. Pant S. et al.,(2024) studied optimized HFS-based WFTS framework that integrates adaptive-radius clustering, hesitant fuzzification, Markov weighting, and Grey Wolf Optimization, enabling unequal interval partitioning, recurrence handling, and superior forecasting accuracy across diverse datasets. Ramkumar M. et al., (2024) profounded about fully convolutional network which is a graph-momentum with modified Elman spike neural networks that enables accurate brain-tumor segmentation with survival prediction, achieving 97% segmentation accuracy while effectively integrating optimized multimodal features. Kordnoori S.et al.,(2024) investigated novel multitask deep-learning framework that integrates shared feature encoding, tumor segmentation, and multilayer perceptron classification to simultaneously delineate and classify meningiomas, gliomas, and pituitary adenomas, achieving 97% accuracy. Devi S.N.et al.,(2024) discussed adaptive Deep Convolutional Neural Network (ADCNN) by incorporating Remora Optimization with MRI-based brain-tumor segmentation having optimizing learning rates, improving feature extraction, and demonstrating superior segmentation performance compared with conventional clustering and CNN approaches. Patil S. et al.,(2026) studied brain tumor classification using MRI, CT, and multimodal fusion, highlighting CNNs, transformers, attention mechanisms, and quantum-inspired models while emphasizing accuracy, interpretability, efficiency, and clinical applicability. Vavekanand R. et al.,(2026) discussed MML (Multimodal Machine Learning) in healthcare, emphasizing fusion strategies, diagnostic improvements, and emerging methods while identifying persistent challenges in data integration, validation, transparency, and clinical deployment.

BraTS (Brain tumor segmentation), comprises the image of glioma datasets, with respect to the datasets from 2013, 2015, 2018, 2019, 2020, and 2021. This gathering of datasets was primarily developed for tumor segmentation challenges but recently employed for binary glioma-grade classification also (Pandey S. et al.,2024). It is considered to be a retrospective

compilation of brain-tumor images acquired using various imaging tools and approaches during standard medical examinations across multiple clinical centers. Consequently, the dataset contains diverse, high-quality images representing several types of medical conditions and processes. The data sequences in which T1, T2, and FLAIR image sequences, are included with MR images corresponding to different glioma condition parameters.

## 2. FORMULATION OF THE PROBLEM

### 2.1 Fuzzy C-Means (FCM)

Initially, Fuzzy C-Means (FCM) is a prominent gathering algorithm for image segmentation in which its application is well known for medical image analysis. By assigning each component hac a proportional membership value, FCM as a soft gathering approach, surpasses conventional method with a more flexible and comprehensive representation in experimental applications. Its worldwide implementation in medical image segmentation focused its ability to distinguish complex elements and patterns with improved accuracy, robustness, and flexibility.

Let $X = \{x_1, x_2, \ldots\ldots, x_n\}$ is finite set of elements and $V = \{v_1, v_2, \ldots\ldots, v_n\}$ is cluster center. The FCM's is objective function i.e.

$$J_{FCM} = \sum_{i-1}^{N} \sum_{j=1}^{C} u_{ij}^{m} \left\| X_i - V_j \right\|^2, \quad (1)$$

where N represents samples, $C$ is clusters, $M$ is Fuzzy Exponent $m > 1$, $X_i = \text{grayscale at i}^{\text{th}}\text{pixel}$, $u_{ij} =_{=}$ membership degree of $X_i$ in cluster J and

$\left\| x_i - y_j \right\|^2$ is Euclidean distance.

The membership function $u_{ij}$ is

$$u_{ij} = \frac{1}{\sum_{k=1}^{c} \left( {\left\| x_i - y_j \right\|^2} / {\left\| x_i - v_k \right\|^2} \right)^{1/(m-1)}}. \quad (2)$$

The cluster center $v_j$ is

$$v_j = \frac{\sum_{i=1}^{n} u_{ij}^{m} x_i}{\sum_{i=1}^{N} u_{ij}^{m}}. \quad (3)$$

Halt condition is $max_{ij} = \{u_{ij}^{k+1} - u_{ij}^{k}\} < \in$,

where, $\in$ represents the finishing/stopping criteria, $K$ denotes the count of iteration.

Beside this, there are several demerits for the employment of FCM including its time taking manner and dependence on membership matrix i.e. starting cluster centers and noise sensitivity. Advanced FCM technique have been elicit a possible solution for the management of these issues by recent studies in the field of healthcare and medicine.

### 2.2 Weighted FCM (WFCM)

The notion of weighted membership degrees is inserted into the conventional Fuzzy C-Means clustering algorithm to develop the WFCM approach. In FCM, each data point is assigned a membership degree for each cluster, which indicates the degree or probability to which the data point belongs to the corresponding cluster. During each iteration of the conventional FCM algorithm, all data points contribute equally to the computation and determination of the cluster centroids. However, WFCM introduces appropriate weighting variables to assign different degrees of importance to individual data points. This weighting mechanism is particularly useful in situations where certain data points possess greater significance than others, thereby allowing the clustering process to give greater influence to more important data elements. The weight parameter's value is

$$U_{ij} = u_{ij} * w_{ij}. \quad (4)$$

The $U_{ij}$is employed to produce a modified membership function in the ambiguous categorizing strategy, which reduces computing challenges. The fuzzy weighting factor $w_{ij}$ in equation (4), incorporates the spatial and intensity distance factor.

$$W_{ij} = w_{is} * w_{sj}. \quad (5)$$

The technique effectively performs the process of clustering by dividing the $'c'$ clusters of the given input data using the $N$ i.e. no. of samples spatial details of the membership function $U_{ij}$cluster center $v_j$.

$$W_{sj} = \frac{1}{1+d_{ij}^{s}}. \quad (6)$$

$$W_{sj} = 1 - log\left(d_{ij}^{I}\right) \quad , \quad (7)$$

where $W_{is}$ = spatial information, $d_{ij}^{s}$ = Spatial Euclidean distance, $W_{sj}$ = intensity information, $d_{ij}^{I}$ = intensity distance.

With comparing the spatial data of adjacent pixels is essential for calculating the Euclidean distance between the cluster centres and the corresponding pixels. WFCM has been proposed as an alternative to the conventional FCM method to overcome the problem of boundary overlapping and with this its local information can be incorporated by considering intensity and spatial functions simultaneously. This technique is particularly beneficial for the segmentation of MR brain images, as it does not introduce speckle noise. Consequently, the combined utilization of intensity and spatial information facilitates a more precise computation of the differences between neighbouring pixels. Pixel weights are incorporated to identify and group the spatial information associated with neighbouring pixels effectively. WFCM ensures greater accuracy in grouping and separating individual pixels into coherent and meaningful clusters. The weight function incorporated with the FCM gathering algorithm is represented as

$$J_{w\,FCM} = \sum_{i=1}^{N}\sum_{j=1}^{C} U_{ij}^{m}\left\|X_i - V_j\right\|^2, \quad (8)$$

To attain optimal classification results, the fuzziness coefficient $'m'$ has been configured to a value of $'2'$.

**2.3 Emperor Penguin Optimization (EPO)**

The behavior pattern of penguins in the wild scenario serves as the learning model for the algorithmic Emperor Penguin Optimization (EPO) approaches. This optimization technique is inspired by the cooperative strategies adopted by penguins to survive the harsh Antarctic winter. EPO is designed to solve universal optimization problems by the mimicking organizational and huddling behavior found within emperor penguin populations (Pant S. et al.,2024). This method has attracted considerable attention because of its effectiveness in addressing multifaceted and complex optimization problems, along with its sharpness and easy handling for implementation. The huddling patterns of penguins(Emperor) forms the basis of the initial and basic phases of EPO, that also include calculation of huddling boundary, temperature, and distance, target to recognize the most efficient mover within the huddle, and subsequently relocating the effective mover (Ramkumar M. et al., 2024).

**Step 2.3.1: Creation and Establishment of Huddle Boundary**

Emperor penguins (EPs) typically form a huddle within a polygon-shaped plane grid boundary during the swarming process. During this process, at least two neighbouring EPs are selected randomly to participate in the swarm. To determine the swarming boundary surrounding the polygon plane, the movement of wind within the swarm is calculated. However, the wind travel at a higher speed than the emperor penguins, and this difference in movement is considered in determining the huddle boundary and subsequent positioning of the penguins.

The huddle boundary of EP that is produced arbitrarily is defined as

$$\psi = \nabla\varphi, \quad (9)$$

where $\varphi$ is velocity of wind.

The complex potential is represented as

$$F = \varphi + i\Omega, \quad (10)$$

Here $F$ is analytical function in polygon plane ,$i$ is fixed value and $\Omega$ *is vector* .

**Step 2.3.2: Determine the huddle's surrounding temperature profile**

In order to optimize the huddle's interior temperature and preserve energy, the EPs generates huddle. To simulate this scenario numerically we assume $T = 0$ , when $R > 1$ and $T = 1$ ,when $R \in 1$. $T$ is temperature, $R$ is polygon's radius, Temperature profile around the huddle is

$$T = \left(T - \frac{MAX_{iterations}}{x - MAX_{iteration}}\right), \quad (11)$$

where, $x$ is current iteration, $MAX_{iteration}$ *is* maximum iteration.

**Step 2.3.3: Calculate the distance among each emperor penguin.**

The solution with the fitness value closest to the optimum is currently the best optimal solution.

The updated positions are listed as

$$\vec{D}_{ep} = \left|S(\vec{A}).\vec{P}(x) - \vec{C}.\overrightarrow{P_{ep}}(x)\right|, \quad (12)$$

Where, $\vec{D}_{ep}$ is distance between the EP and the best fitted search agent, $\vec{A}$ and $\overrightarrow{C}$ represents avoiding collision between neighbors, $\overrightarrow{P}$ is best optimal solution, $\overrightarrow{P_{ep}}(x)$ is position vector of EP. Here

$$A = \left(M * \left(T + P_{grid}(Accuracy)\right)\right) * Randomvalue\text{-}T, \quad (13)$$

$$P_{grid}(Accuracy) = \left|\vec{P} - \vec{P}_{ep}\right|, \quad (14)$$

$$\vec{c} = Rand(), \quad (15)$$

The function S () is estimated as

$$S(\vec{A}) = \left(\sqrt{\left(f.e^{x/l} - e^{-x}\right)}\right)^2 , \quad (16)$$

**Step 2.3.4: Relocate the mover**

The Eps position is revised based on the optimal solution found through the best available.

$$\vec{P}_{ep}(x+1) = \vec{P}(x) - \vec{A}.\vec{D}_{ep}, \quad (17)$$

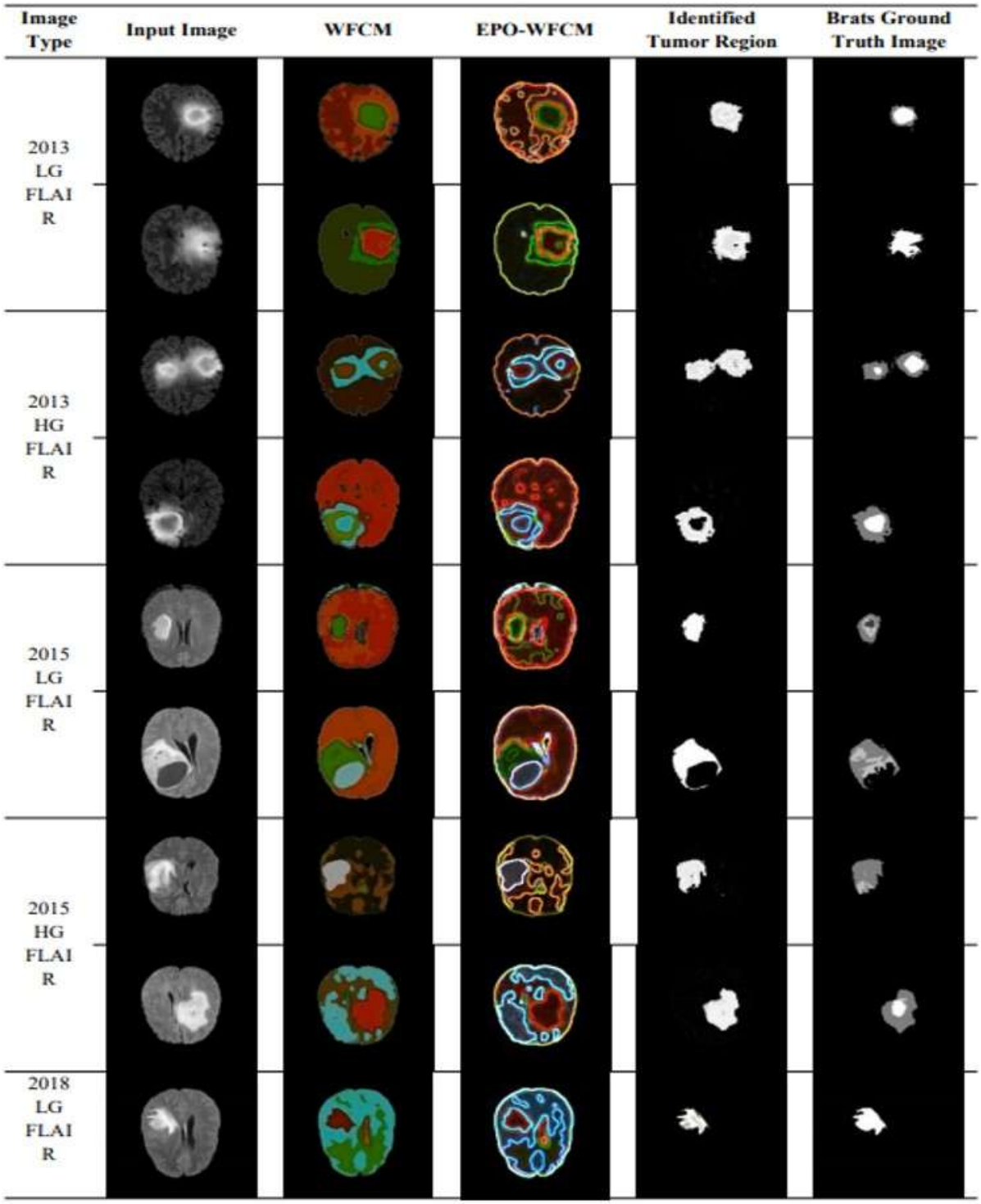
Where, $\vec{P}_{ep}(x+1)$ is Next updated position of EP.

## 3. RESULTS AND DISCUSSION

The proposed chimeric methodology is utilized for the effective recognition and classification of brain tumors in MR images by integrating WFCM (Weighted Fuzzy C-Means) clustering with EPO (Emperor Penguin Optimization). WFCM facilitates the partitioning of MR images into multiple clusters by grouping pixels according to their characteristics and intensity patterns. Furthermore, incorporating EPO into the WFCM clustering framework optimizes the clustering process, minimizes boundary overlap, and reduces uncertainty during segmentation.

The resulting EPO-WFCM segmented images clearly delineate the outer boundaries of individual clusters, thereby enabling accurate discrimination between tumor-affected and non-tumor regions within MR brain images. The combined strategy enhances the precision, consistency, and reliability of tumor localization and segmentation by exploiting the clustering capability of WFCM and the optimization strength of EPO. Figure 4 presents the dispersion results of the MR brain images

obtained using the proposed EPO-WFCM technique, demonstrating its effectiveness in accurately identifying and separating tumor regions.



Natural Resources for Human Health
eISSN: 2583-1194

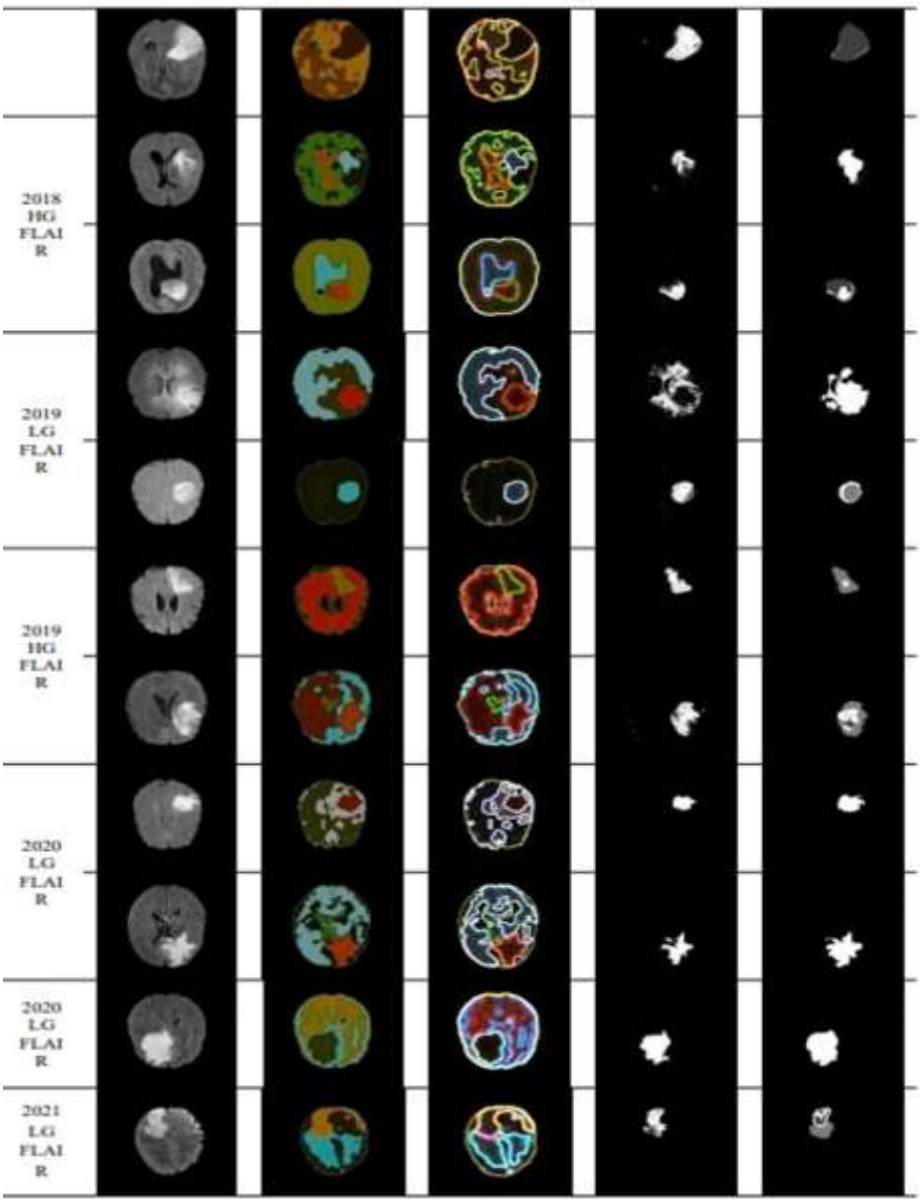



**Figure 4.** Tumor delineation using EFO-WFCM technique

**Table 2.** Performance value of EFO-WFCM

| DATA | TIME | MSE | PSNR | TC | DS |
|---|---|---|---|---|---|
| **2013 LG** | 21.48 | 0.3933 | 52.2181 | 76.1360 | 83.6348 |
| | 23.63 | 0.3600 | 52.6020 | 76.4427 | 84.6486 |
| **2013 HG** | 22.03 | 0.3902 | 52.2523 | 77.7074 | 84.0087 |
| | 22.57 | 0.3830 | 52.3333 | 75.5480 | 85.4570 |
| **2015 LG** | 19.19 | 0.3803 | 52.3639 | 75.7046 | 83.1926 |
| | 20.88 | 0.3874 | 52.2829 | 75.2475 | 83.9593 |
| **2015 HG** | 21.20 | 0.3913 | 52.2397 | 75.7046 | 83.1926 |

| | | | | | |
|---|---|---|---|---|---|
| | 22.67 | 0.3658 | 52.5320 | 75.2475 | 83.9593 |
| **2018 LG** | 20.71 | 0.3944 | 52.2059 | 77.2492 | 85.0837 |
| | 21.81 | 0.3674 | 52.5140 | 77.9571 | 84.9582 |
| **2018 HG** | 20.80 | 0.3842 | 52.3188 | 77.7930 | 86.7826 |
| | 22.15 | 0.3594 | 52.6085 | 76.2992 | 83.1313 |
| **2019 LG** | 22.24 | 0.3698 | 52.4849 | 76.1543 | 86.0518 |
| | 21.75 | 0.3782 | 52.3876 | 75.5691 | 83.9059 |
| **2019 HG** | 19.12 | 0.3596 | 52.6063 | 76.0070 | 86.8621 |
| | 20.88 | 0.3964 | 52.1834 | 76.3748 | 83.5855 |
| **2020 HG** | 19.12 | 0.3596 | 52.6063 | 76.0070 | 86.8621 |
| | 20.88 | 0.3964 | 52.1834 | 76.3748 | 83.9059 |
| **2020 LG** | 23.21 | 0.3814 | 52.3511 | 77.3589 | 84.8067 |
| | 19.23 | 0.3922 | 52.2300 | 76.8949 | 85.0916 |
| | 22.59 | 0.3704 | 52.4783 | 75.3858 | 84.5679 |
| **2021 LG** | 19.60 | 0.3630 | 52.5654 | 76.5300 | 85.0269 |
| **AVERAGE** | 21.39 | 0.38 | 52.39 | 76.54 | 84.86 |

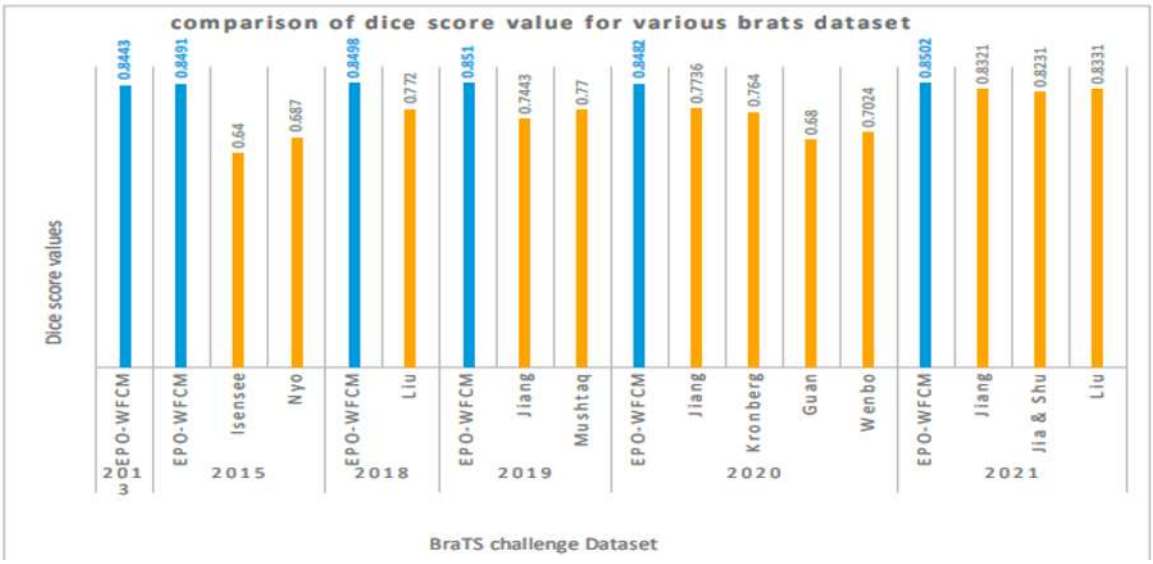



**Figure 5.** Comparison of Dice Score

The efficacy of the suggested EPO-WFCM algorithms was assessed utilizing several activity measures, including the TC (Tanimoto coefficient), DS (Dice score), MSE (Mean squared Error), PSNR (Peak Signal-to-Noise Ratio), and computational time. The segmentation outcome obtained by tell apart tumor-affected with non-tumor regions in MR brain images are presented in the corresponding figure. The proposed technique achieved an average computational time of 21.39 seconds, with MSE, PSNR, TC, and DS values of 0.38, 52.39 dB, 76.54%, and 84.86%, respectively, demonstrating its effectiveness in accurately segmenting tumor regions.

The experimental analysis further compares the performance of the IMV-FCM algorithm with several existing segmentation techniques. Different levels of Gaussian noise were introduced into the images to examine the robustness and noise-handling capability of the suggested algorithm. In the segmentation or dispersion results, A, B, and C indicate about white matter (WM), gray matter (GM), and cerebrospinal fluid (CSF), respectively. Its results indicate that the multi-view approach provides substantially improved segmentation performance compared with conventional FCM when applied to original brain images. By exploiting complementary information from multiple views, the proposed strategy improves the accuracy and reliability of the clustering process.

Furthermore, the IMV-FCM approach demonstrates improved segmentation performance compared with previously developed multi-view clustering techniques. Unlike Co-FKM and Comb KM, which require users to manually determine the parameters associated with combining different data partitions, IMV-FCM adaptively determines the contribution of individual views. This adaptive weighting mechanism enables the method to assign more appropriate view weights during multi-view learning, thereby improving the quality of the resulting clusters and achieving more accurate and robust multi-view image segmentation outcomes.

## 4. CONCLUSIONS

EPO (Emperor Penguin Optimizer) is a population-based meta-heuristic algorithm directed by the collective swarming behavior patterns of emperor penguins. It adjusts the positions of candidate solutions to achieve an effective balance between exploration and exploitation during optimization. In this study, EPO is integrated with WFCM (Weighted Fuzzy C-Means) to improve brain tumor dispersion from MR images. WFCM incorporates spatial information and weighted membership values to distinguish tumor tissues from surrounding regions, while EPO optimizes the clustering process and reduces segmentation ambiguity near tumor boundaries. The proposed EPO-WFCM framework is evaluated using several BraTS datasets and compared with corresponding ground-truth images. Experimental observations indicate improved tumor-region separation and boundary identification. The proposed approach can assist medical practitioners by enabling faster tumor detection, supporting treatment planning, and improving the efficiency of computer-aided brain image analysis.

**Data generation statement**: All data generated or analyzed during the current investigation are added inside the manuscript.

**Competing interest of authors**: Authors have no competing interest.

**Funding agency**: This work was not supported by any funding agency.

## REFERENCES

[1] Barman U, Choudhury RD, Sahu D, Barman GG (2020), "Comparison of convolution neural networks for smartphone image based real time classification of citrus leaf disease," *Comput Electron Agric* 177:105661

[2] Chen D, Shi Y, Huang W, Zhang J, Wu K (2018), "Mapping wheat rust based on high spatial resolution satellite imagery," *Comput Electron Agric* 152:109–116.

[3] Chen CJ, Huang YY, Li YS, Chang CY, Huang YM (2020), "An AIoT based smart agricultural system for pests' detection," *IEEE Access* 8:180750–180761.

[4] Devi, S.N., Gnanamanoharan, E. and Chinnadurai, M., 2024. BrainTumour Segmentation Using Adaptive Deep Convolutional NeuralNetwork System.International Journal of Intelligent Systems andApplications in Engineering, 12(3s), pp.179-189.

[5] Deng L, Wang Y, Han Z, Yu R (2018), "Research on insect pest image detection and recognition based on bio-inspired methods," *Biosystem Eng* 169:139–148.

[6] Deng X, Huang Z, Zheng Z, Lan Y, Dai F (2019), "Field detection and classification of citrus huanglongbing based on hyperspectral reflectance," *Comput Electron Agric* 167:105006.

[7] Dhiman,G., Kumar, V.,2018. Emperor penguin optimizer: Abio-inspired algorithm for engineering problems. *Knowledge-Based Systems*, 159, pp.20-50.

[8] Dhingra G, Kumar V, Joshi HD (2019), "A novel computer vision-based neuromorphic approach for leaf disease identification and classification, "*Measurement* 135:782–794.

[9] Jamazi, C., Manita, G., Chhabra, A., Manita, H. and Korbaa, O.,2024. Mutated Aquila Optimizer for assisting brain tumor segmentation. *Biomedical Signal Processing and Control*, 88,p.105089.

[10] Kordnoori, S., Sabeti, M., Shakoor, M.H. and Moradi, E., 2024. Deep multi-task learning structure for segmentation and classification of supratentorial brain tumors in MR images. *Interdisciplinary Neurosurgery*, 36, p.101931.

[11] Pant, S. and Kumar, S., 2024. HFS-based computational method for weighted fuzzy time series forecasting model using techniques of adaptive radius clustering and grey wolf optimization. *Granular Computing*, 9(1), p.11.

[12] Pandey, S., Changdar, S., Perslev, M. and Dam, E.B., 2024. Fully Automated Tumor Segmentation for Brain MRI data using Multiplanner UNet. arXiv preprint arXiv:2401.06499.

[13] Patil, S. and Gavade, P., 2026. Improving brain tumor diagnosis: A systematic review of CT, MRI, and fusion-based deep learning models. Imaging, Online First.

[14] Qiu, C., Song, Y., Liu, Y., Zhu, Y., Han, K., Sheng, V.S. and Liu, Z.,2024. MMMViT: Multiscale multimodal vision transformer for brain tumor segmentation with missing modalities. *Biomedical Signal Processing and Control*, 90, p.105827.

[15] Ramaraj, K., Govindaraj, V., Zhang, Y.D., Murugan, P.R., Wang, S.H., Thiyagarajan, A. and Sankaran, S., 2022a. Agnostic multimodal brain anomalies detection using a novel single-structured framework for better patient diagnosis and therapeutic planning in clinical oncology. *Biomedical Signal Processing and Control*, *77*, p.103786.

[16] Ramaraj, K., Amiya, G., Rajasekaran, M.P., Govindaraj, V., Vasudevan, M., Thirumurugan, M., Zhang, Y.D., Abdullah, S.S. and Thiyagarajan, A., 2023b. A robust multi-utility neural network technique integrated with discriminators for bone health decisioning to facilitate clinical-driven processes. *Research on Biomedical Engineering*, *39*(1), pp.139-157.

[17] Ramkumar, M., Kumar, R.S., Padmapriya, R. and Karthick, S., 2024.Brain tumor segmentation and survival time prediction using graph momentum fully convolutional network with modified Elman spike neural network. *International Journal of Imaging Systems and Technology*, 34(1), p.e23005.

[18] Sakli, M., Essid, C., Salah, B.B. and Sakli, H., 2024. Deep Learning Methods for Brain Tumor Segmentation. In *Machine Learning and Deep Learning Techniques for Medical Image Recognition* (pp. 168-193). CRC Press.

[19] Vavekanand, R., Kumar, T., Kumar, S., Kumar, G. and Laghari, A.A., 2026. Multimodal Machine Learning Approaches in Predictive Healthcare Analytics: A Comprehensive Survey. *Archives of Computational Methods in Engineering*, 33, pp.7667-7691.

[20] Yu, H., Jiang, L., Fan, J., Xie, S. and Lan, R., 2024. A feature-weighted suppressed possibilistic fuzzy c-means clustering algorithm and its application on color image segmentation. *Expert Systems with Applications*, 241, p.122270.